



2001012634
533131
10/05

AIAA 2001-2266

**Comparison of Two Acoustic Waveguide
Methods for Determining Liner
Impedance**

Michael G. Jones, Willie R. Watson,
Maureen B. Tracy, and Tony L. Parrott
NASA Langley Research Center
Hampton, VA

**7th AIAA/CEAS
Aeroacoustics Conference
May 28-30, 2001
Maastricht, The Netherlands**

Comparison of Two Acoustic Waveguide Methods for Determining Liner Impedance

Michael G. Jones,* Willie R. Watson,[†] Maureen B. Tracy,[‡] and Tony L. Parrott[§]
NASA Langley Research Center
Hampton, VA

Abstract

Acoustic measurements taken in a flow impedance tube are used to assess the relative accuracy of two waveguide methods for impedance eduction in the presence of grazing flow. The aeroacoustic environment is assumed to contain forward and backward-traveling acoustic waves, consisting of multiple modes, and uniform mean flow. Both methods require a measurement of the complex acoustic pressure profile over the length of the test liner. The Single Mode Method assumes that the sound pressure level and phase decay rates of a single progressive mode can be extracted from this measured complex acoustic pressure profile. No *a priori* assumptions are made in the Finite Element Method regarding the modal or reflection content in the measured acoustic pressure profile. The integrity of each method is initially demonstrated by how well their no-flow impedances match those acquired in a normal incidence impedance tube. These tests were conducted using ceramic tubular and conventional perforate liners. Ceramic tubular liners were included because of their impedance insensitivity to mean flow effects. Conversely, the conventional perforate liner was included because its impedance is known to be sensitive to mean flow velocity effects. Excellent comparisons between impedance values educed with the two waveguide methods in the absence of mean flow and the corresponding values educed with the normal incident impedance tube

were observed. The two methods are then compared for mean flow Mach numbers up to 0.5, and are shown to give consistent results for both types of test liners. The quality of the results indicates that the Single Mode Method should be used when the measured acoustic pressure profile is clearly dominated by a single progressive mode, and the Finite Element Method should be used for all other cases.

Nomenclature

c	sound speed in duct, m/s
f	frequency, Hz
H	duct height, m
i	$= \sqrt{-1}$
k	free space wavenumber, m^{-1}
k_x	axial wavenumber for single progressive mode, m^{-1}
k_y	transverse wavenumber, m^{-1}
L	length of FEM computational domain, m
L_1, L_2	distance from source plane to liner leading and trailing edges, respectively, m
M	average Mach number across duct cross-section
$p(x, y)$	complex acoustic pressure, Pa
p_{ref}	reference pressure, 20 μ Pa
SPL(x)	sound pressure level, dB
x, y	axial and transverse coordinates, respectively, m
x_i	wall measurement location, m

Symbols:

$\phi(x)$	measured phase, radians
ρ_0	ambient density
θ	acoustic resistance, real component of ζ
ω	$= 2\pi f$, angular frequency
χ	acoustic reactance, imaginary component of ζ
ζ	$\theta + i\chi$, normal incidence acoustic impedance, normalized by $\rho_0 c$

*Research Scientist, Structural Acoustics Branch, Aerodynamics, Aerothermodynamics and Acoustics Competency

[†]Senior Research Scientist, Computational Modeling and Simulation Branch, Aerodynamics, Aerothermodynamics and Acoustics Competency, Member of AIAA

[‡]Research Scientist, Aeroacoustics Branch, Aerodynamics, Aerothermodynamics and Acoustics Competency

[§]Senior Research Scientist, Structural Acoustics Branch, Aerodynamics, Aerothermodynamics and Acoustics Competency

Copyright ©2001 by the American Institute of Aeronautics and Astronautics, Inc. No copyright is asserted in the United States under Title 17, U.S. Code. The U.S. Government has a royalty-free license to exercise all rights under the copyright claimed herein for government purposes. All other rights are reserved by the copyright owner.

Introduction

The continual improvement of acoustic liner design is a critical element in commercial aircraft noise emission control. To that end, it is becoming increasingly important to achieve the optimum liner impedance for each portion of the engine nacelle. To achieve this goal, test methodologies must be established to accurately educe the normal incidence acoustic impedance of test liners in the presence of mean flow. This knowledge can then be used to improve the existing acoustic impedance prediction tools, such that additional liner configurations can be confidently predicted without the need for costly experimental tests. Typically, either *in situ*¹ or waveguide^{2,3} methods are used to educe the acoustic impedance of test liners.

The *in situ* method requires the insertion of two microphones into the test liner. (Additional microphones are required for multi-layer liners.) The transfer function between the complex acoustic pressures measured by these microphones is then used to educe the acoustic impedance. This method is simple to implement; however, there are a few drawbacks. In addition to microphone installation effects (local damage to the liner by microphone insertion and discontinuous surface impedance due to a flush-mounted microphone in the liner), the *in situ* method provides only local information. In order to determine if the liner exhibits a uniform impedance, this method must be applied a number of times with the microphones installed at various locations in the liner. Regardless, because of its simplicity, the *in situ* method remains quite useful.

Waveguide methods, on the other hand, provide global results without the need for invasive measurements within the test material. However, they typically require significantly more data than is needed for the *in situ* method. Depending on the complexity of the chosen implementation, waveguide methods can be used to analyze uniform or variable impedance liners, sometimes with the same data acquisition sequence.

The purpose of this paper is to assess the integrity of two waveguide methods for determining the normal incidence acoustic impedance in grazing flow. The aeroacoustic environment is assumed to contain forward and backward-traveling acoustic waves, consisting of multiple modes, and uniform mean flow. Both methods require a measurement of the complex acoustic pressure profile over the length of the liner. The Single Mode Method (SMM) is based on the assumption that the sound pressure level and phase decay rates of a single progressive mode can be ex-

tracted from this measured acoustic pressure profile data. The Finite Element Method (FEM) makes no *a priori* assumptions regarding the modal content or the amount of reflections in the measured data. The integrity of each method is initially demonstrated by showing agreement between their impedance values educed in the absence of flow and those acquired in a normal incidence impedance tube. The two methods are then compared for tests with up to Mach 0.5 mean flow.

The remainder of this paper is organized into four sections. The first section gives a description of the waveguide and test liners, and describes the data acquisition system for the two impedance eduction methodologies. The second section provides a brief discussion of the theory underlying the two waveguide methods. The third section contains a discussion of the results obtained after implementation of the two impedance methodologies on data acquired in the NASA Langley Flow Impedance Test Facility. Conclusions relevant to this paper are presented in the final section.

Experimental Setup

Description of Test Liners

Two types of acoustic liners were used in the current study; ceramic tubular and conventional perforate. The ceramic tubular material was chosen because it is expected to be insensitive to mean flow effects. Sensitivity to mean flow velocity is expected to be significantly increased for the conventional perforate liner, for which the acoustic resistance is concentrated in the vicinity of the orifices. The two liner types, shown schematically in figure 1, are described in detail here:

- a) The ceramic tubular liner consists of "sinusoid-shaped" parallel channels embedded in a ceramic matrix. These channels, with equivalent circular diameters of 0.76 mm, run perpendicular to the exposed surface to provide a surface porosity of 65%. The channels are rigidly terminated such that each is isolated from its neighbor to ensure a locally reacting structure. The channel diameter is small enough that the flow effects are minimal without the typical addition of a cover sheet.

Three ceramic tubular configurations were tested. The first was a uniform-depth configuration, in which all channels were 77.5 mm deep. For convenience, this liner is labeled "CT1". For the other two configurations, labeled "CT2" and "CT3", the channel depth was varied over a 50.8 mm length (1/8th of total length) of

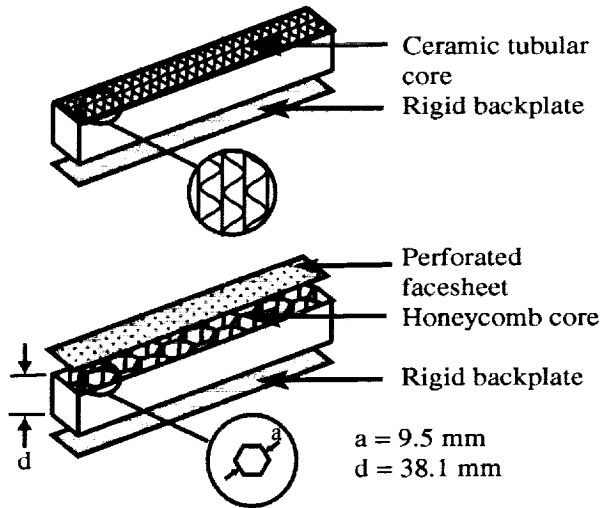


Fig. 1. Sketch of test liners.

the liner. This pattern was repeated over the entire length of the liner (8 cycles). The dimensions for these configurations are included with the sketch in figure 2. A prediction code⁴ was used with an optimization routine to determine the channel depths and "step" lengths for the "CT2" liner (staircase pattern), with a target impedance of $\rho_0 c$. A quadratic residue sequence⁵ was used as a guide in the design of the "CT3" liner. This design is commonly used in concert halls to improve listener response.

Clearly, the impedance should vary along the length of the liner for the "CT2" and "CT3" configurations, since the depth of each liner varies in the axial direction. Since a full cycle of depth variation occurs within a 50.8 mm length, which is less than the shortest wavelength of interest, the impedance is assumed to be "smeared" over the surface of the liner. It should also be noted here that the FEM described in this paper is capable of resolving this impedance variability. However, the amount of data required increases as the impedance variability to be resolved increases.

- b) The perforate liner consists of an aluminum facesheet bonded onto 9.5 mm-diameter hex-cell honeycomb cavities that are 38.1 mm in depth. The facesheet has a porosity of 8.7%, with 0.1 mm-diameter holes and a sheet thickness of 0.64 mm. This liner is typical of the type of material currently installed in commercial aircraft engines for noise suppression.

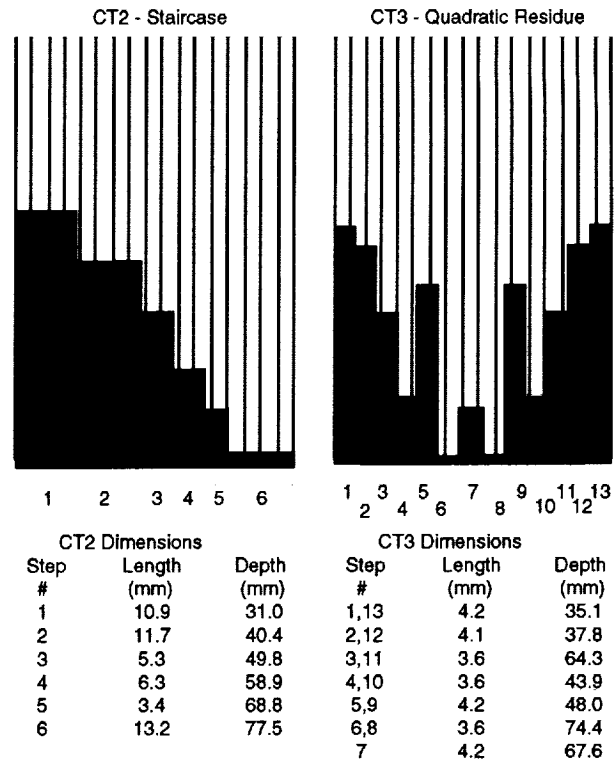
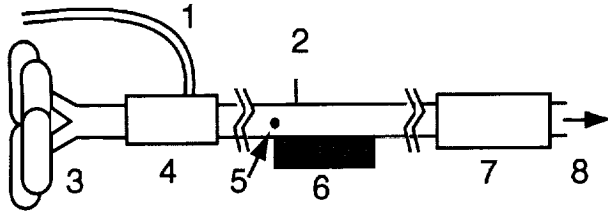


Fig. 2. Sketch of "CT2" & "CT3" - 1 cycle.

Test Apparatus and Data Acquisition

The input data used to educe the impedances of each liner were obtained from measurements in the NASA Langley Flow Impedance Test Facility. A schematic of the flow impedance tube is provided in figure 3. This apparatus has a 50.8 mm x 50.8 mm cross-section in which a controlled aeroacoustic environment is achieved. The 50.8 mm-wide by 406.4 mm-long liner is centered in a test section that includes the region from the source plane (203.2 mm upstream of the liner leading edge) to the exit plane (203.2 mm downstream of the liner trailing edge).

The desired aeroacoustic environment in the test section is achieved with four 120 Watt electromagnetic acoustic drivers, whose phase-matched outputs are combined to generate discrete tones from 0.5 to 3.0 kHz with sound pressure levels of 130 dB at the liner leading edge. The mean flow is conditioned by a specially designed plenum that allows flow to be combined with the sound field such that sound transmission efficiency degradation is minimal. The uniform flow Mach number used to perform each impedance eduction in this report was taken to be the average value of the Mach number profile measured at the mid-liner axial plane (406.4 mm downstream of the source plane). Tests were conducted



1. High pressure air line
2. Traversing microphone
3. Acoustic drivers
4. Plenum
5. Reference microphone
6. Test section with liner
7. Termination
8. To vacuum pumps

Fig. 3. LaRC Flow Impedance Tube.

for centerline Mach numbers of 0.0, 0.1, 0.3 and 0.5.

Acoustic waves propagate from left to right in figure 3, traversing the surface of the test specimen, and into a termination section designed to minimize reflections over the frequency range of interest. Two 6.35 mm condenser-type microphones are flush mounted in the test section; a reference microphone at the test specimen leading edge on the side wall and a traversing microphone on an axial traverse bar, which forms a portion of the upper wall of the test section. A 13.0 mm-wide precision-machined slot in the top wall of the flow impedance tube allows this axial traverse bar to traverse the test section length by means of a computer-controlled digital stepping motor. The data acquisition program automatically positions the traversing microphone at pre-selected locations, x_i , from 203.2 mm upstream of the leading edge to 50.8 mm downstream of the trailing edge of the liner. At each measurement location, a transfer function between the traversing and reference microphones is used to determine the sound pressure level $SPL(x_i)$ and phase $\phi(x_i)$ relative to the fixed microphone location. The complex acoustic pressure at a given axial wall location is determined from the equation

$$p(x_i, H) = p_{\text{ref}} 10^{SPL(x_i)/20} e^{i\phi(x_i)} \quad (1)$$

where the reference pressure, p_{ref} , is 20 μPa . It should be noted that an $e^{i\omega t}$ time convention is used throughout this paper.

The source-plane acoustic pressure and exit-plane impedance are typically functions of location in these planes. Therefore, transverse probe microphones should be used to measure this data with the test liner installed. However, the flow impedance

tube used in this study was designed to be operated with source frequencies below the cut-on frequency of higher-order modes. Also, the cross-section of the tube is such that the insertion of probes causes concerns regarding blockage effects. To eliminate the need to install transverse probes, the experiment was carefully designed to minimize higher-order mode effects at the source and exit planes. However, higher-order mode effects cannot be avoided in the liner region. These higher-order modes, as well as reflections, are generally present in the vicinity of the leading and trailing edges of the specimen.

To avoid the need for a transverse probe, the source plane was located 203.2 mm upstream of the leading edge of the test specimen in the hardwall section of the duct, and the source frequency was kept below the cut-on frequency of higher-order hardwall modes. Higher-order mode effects caused by the installation of the test specimen are expected to decay upstream of the leading edge of the test specimen. Therefore, the source pressure at each point along the source plane is set to the value measured at the upper wall source location.

A similar procedure is applied at the exit plane. The exit plane is located 203.2 mm downstream of the trailing edge of the test specimen, also in the hardwall section of the duct. A rotating two-microphone plug was installed in the duct sidewall near the exit plane, and the switched two-microphone method⁶ was used to obtain the exit impedance. Because the exit plane is 4 duct heights downstream of the trailing edge of the liner, higher-order modes generated by the installation of the liner are not expected to carry appreciable acoustic energy to the exit plane. Thus, the exit impedance values at all points in the exit plane are assumed identical.

Acoustic Waveguide Methods

Single Mode Method (SMM)

The SMM uses an infinite-waveguide model to reduce the impedance of the test liner from the measured wall complex acoustic pressure profile for a single, unidirectional propagating mode.² The maximum frequency tested was 3.0 kHz, which is typically below the cut-on frequency of higher-order hardwall modes for the flow duct used in this study. The one exception to this is for Mach 0.5 mean flow, for which the cut-on frequency is reduced to approximately 2.9 kHz. At this Mach number, data acquired at 3.0 kHz can potentially contain one higher-order mode in the hardwall section. Exploratory tests conducted at higher frequencies, however, have previ-

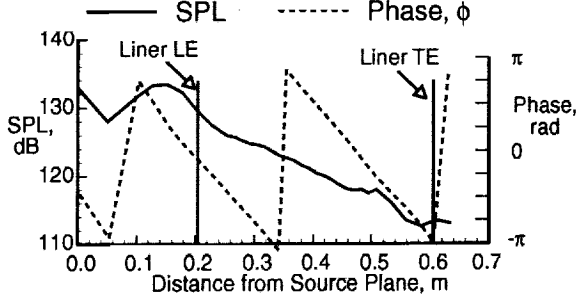


Fig. 4. Sample SPL & phase profiles.

ously indicated that this higher-order mode is not carrying significant energy. Thus, potential higher-order mode effects in the hardwall region were ignored for this study.

For this method, that portion of the measured complex acoustic pressure profile which is over the liner but away from the liner leading and trailing edges is used. For the current study, this distance was typically set at approximately 50.8 mm, or one duct height. Thus, only the measured upper-wall acoustic pressure profile which was over the central portion (approximately 305 mm) of the liner was used in the analysis. Figure 4 displays sound pressure level (SPL) and phase (ϕ) data measured along the upper wall of the NASA Langley Flow Impedance Tube. The standing wave patterns in the SPL data near the leading and trailing edges of the liner indicate that reflections and/or high-order mode effects are contaminating that portion of the data. For the central portion of the data, however, the SPL and phase decay with easily identifiable linear slopes. This is an indication that a single, progressive mode is dominant over the central portion of the liner. The SMM uses data from the central portion of the curve to educe the impedance of the test liner, assuming a single progressive mode.

The details of the SMM are provided in detail elsewhere.² For convenience, the elements necessary to use the method are repeated here. First, the axial wavenumber (k_x) for the dominant progressive mode is computed from the measured portion of the data that has a constant slope using

$$k_x = \frac{d\phi(x)}{dx} + \frac{i}{20 \text{Log}_{10}(e)} \frac{d\text{SPL}(x)}{dx} \quad (2)$$

In our selected time convention ($e^{i\omega t}$), the signs of $\frac{d\text{SPL}(x)}{dx}$ and $\frac{d\phi(x)}{dx}$ are assumed to be negative for right moving waves. The normal incidence acoustic

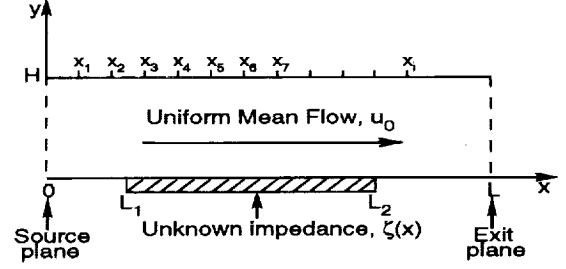


Fig. 5. Geometry and coordinate system for FEM. (Not to scale)

impedance of the liner can then be determined using

$$\zeta = -i \frac{k}{k_y} \left(1 - M \frac{k_x}{k} \right)^2 \cot \left[(kH) \left(\frac{k_y}{k} \right) \right] \quad (3)$$

where

$$\frac{k_y}{k} = \frac{1 - [(1 - M^2) \left(\frac{k_x}{k} \right) + M]^2}{(1 - M^2)} \quad (4)$$

Finite Element Method (FEM)

Figure 5 depicts the applicable geometry and coordinate system used to model the flow duct test section for the FEM. This method is described in detail elsewhere³ and only sufficient detail is presented here for completeness. The version of the FEM used in this study incorporates the assumptions that the mean flow profile is uniform and only plane acoustic waves exist in the spanwise direction (not shown in the sketch). The maximum frequency (3.0 kHz) is below the cut-on frequency for higher-order modes in a hardwall region for all but the highest Mach number ($M=0.5$) tested. In the lined section, the two side walls are rigid; thus, the assumption of no higher-order modes in the spanwise direction is reasonable for the frequency range of interest.

The regions upstream ($x = 0$ to L_1) and downstream ($x = L_2$ to L) of the liner contain rigid walls. As described earlier, the complex acoustic pressures are measured at each of the measurement locations located along the upper wall (at $x = 0, x_1, x_2, \dots, x_i$) using a microphone flush-mounted in the traversing bar.

The FEM finds the solution to the steady-state form of the convected wave equation,

$$(1 - M^2) \frac{\partial^2 p}{\partial x^2} + \frac{\partial^2 p}{\partial y^2} - 2ikM \frac{\partial p}{\partial x} + k^2 p = 0 \quad (5)$$

The source plane acoustic pressure boundary condition is

$$p(0, y) = p_s(y) \quad (6)$$

where $p_s(y)$ is the acoustic pressure profile in the transverse direction at the source plane. Because only plane waves are assumed at the source plane, $p_s(y)$ is set to the constant value measured with the traversing microphone positioned in the source plane.

The exit plane boundary condition is

$$\frac{\partial p(L, y)}{\partial x} = \frac{-ikp(L, y)}{M + \zeta_{\text{exit}}(y)} \quad (7)$$

which is derived from the requirement that the exit impedance, $\zeta_{\text{exit}}(y)$, must equal the ratio of the acoustic pressure to the axial component of acoustic velocity in that plane. Since only plane acoustic waves are assumed at the exit plane, ζ_{exit} is taken to be the constant value determined using flush-mounted measurements and plane wave analysis.⁶ The boundary conditions at all rigid walls are given as

$$\frac{\partial p}{\partial y} = 0 \quad (8)$$

which indicates that the normal component of acoustic particle velocity vanishes at a rigid wall. Finally, the boundary condition for the lined region of the duct (from $x = L_1$ to $x = L_2$ in figure 5) is given by³

$$\frac{\partial p(x, 0)}{\partial y} = \frac{ikp(x, 0)}{\zeta(x)} + 2M \frac{\partial}{\partial x} \left[\frac{p(x, 0)}{\zeta(x)} \right] + \frac{M^2}{ik} \frac{\partial^2}{\partial x^2} \left[\frac{p(x, 0)}{\zeta(x)} \right] \quad (9)$$

Equations (5)-(9) constitute a boundary value problem that can be solved to obtain the upper wall pressure when the impedance of the liner, $\zeta(x)$, is known. The goal of the FEM is to determine the unknown liner impedance, $\zeta(x)$, from the measured boundary data. The procedure consists of iterating through the solution to the boundary value problem described by equations (5)-(9), and obtaining a set of upper wall acoustic pressures for each impedance function. As each new set of wall pressures is computed, it is compared to the measured values until convergence is achieved within an acceptable error range.

Results and Discussion

The initial acoustic waveguide method assessment was conducted using the uniform-depth ceramic and perforate liners. These liners were first tested with the NASA Langley Research Center normal incidence impedance tube (NIT).⁷ Figures 6 and 7 contain the acoustic impedances (denoted with “+”

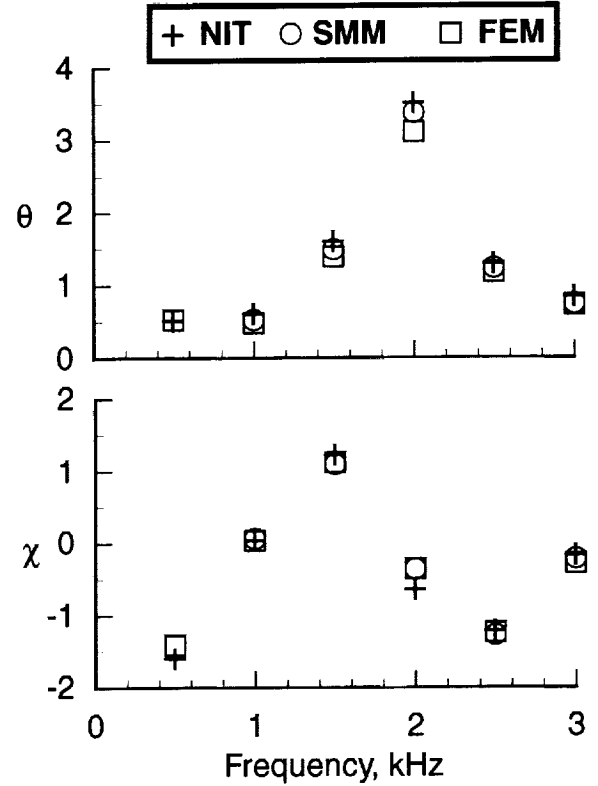


Fig. 6. Ceramic liner “CT1” - no flow.

signs) for each of the liners at frequencies of 0.5 to 3.0 kHz, in steps of 0.5 kHz. Each of these liners was then mounted in the flow impedance tube and tested with no mean flow. The acquired data were analyzed using the SMM and FEM, and the results are included in figures 6 and 7.

For the ceramic liner, the SMM and FEM results (depicted with circles and squares, respectively) are well matched to the corresponding NIT results. The same comparison holds for the perforate liner, except at 0.5 kHz. While the acoustic reactances are still well matched at this frequency, the acoustic resistances are significantly different. Diagnostic tests are planned to try to resolve the discrepancy at this frequency. Similar tests with other liner configurations (not included in this report for the sake of brevity) provided further confirmation that the SMM and FEM reduce the correct impedance spectra in the absence of mean flow.

Next, all four liners (three ceramic and one perforate) were tested in the flow impedance tube at centerline Mach numbers of 0.1, 0.3 and 0.5. The results are provided in figures 8, 9, 10 and 11. As expected, the acoustic resistance sensitivity to mean flow velocity is less for the ceramic liners than for the

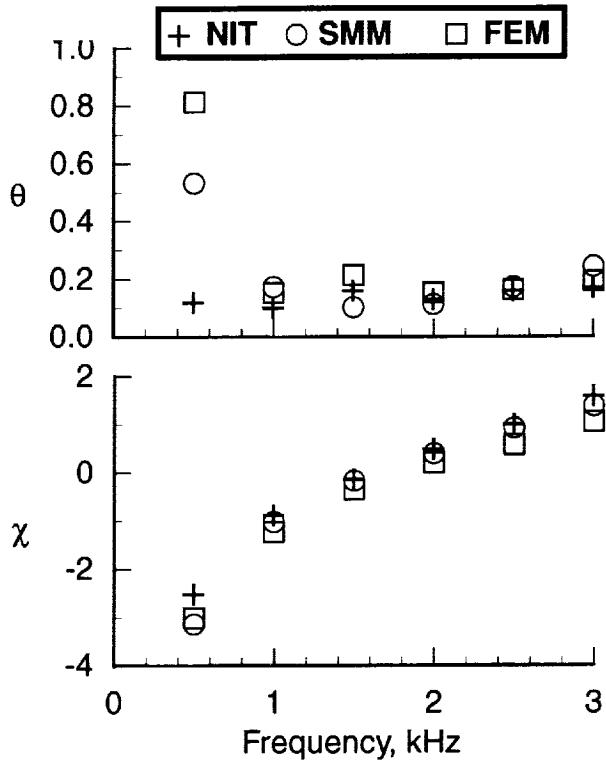


Fig. 7. Perforate liner - no flow.

perforate, except at 0.5 kHz (see earlier discussion). Also, the acoustic resistance is sensitive to mean flow velocity for the uniform-depth ceramic liner near the anti-resonance (2.2 kHz).

There were some conditions where the SMM was not applicable because a region of linear decay of SPL and phase could not be extracted from the data. For the remaining data, the SMM and FEM results are typically well matched.

Figures 8, 9 and 10 contain educed impedances for the three ceramic tubular liner configurations. The "CT1" (uniform depth) impedance spectrum is typical of a "quarter-wavelength" liner, with a resonance near 1 kHz and an anti-resonance near 2 kHz. At 0.5 kHz, the SMM could not be implemented because of significant reflections in the upper-wall acoustic pressure profile. The FEM results at this frequency vary significantly with mean flow Mach number. As stated earlier, further studies are planned to better understand this result. It should be noted, however, that this discrepancy at 0.5 kHz does not occur for all tests. One possible explanation for the discrepancy is that the sensitivity to mean shear flow is increased at low frequencies for highly reflective conditions.⁸ The SMM and FEM results are well matched for the other fre-

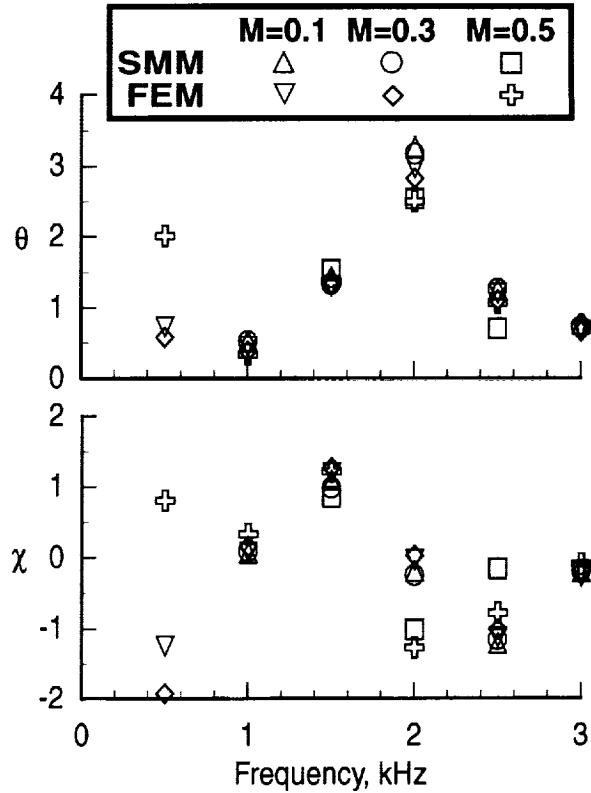


Fig. 8. Ceramic liner "CT1" with flow.

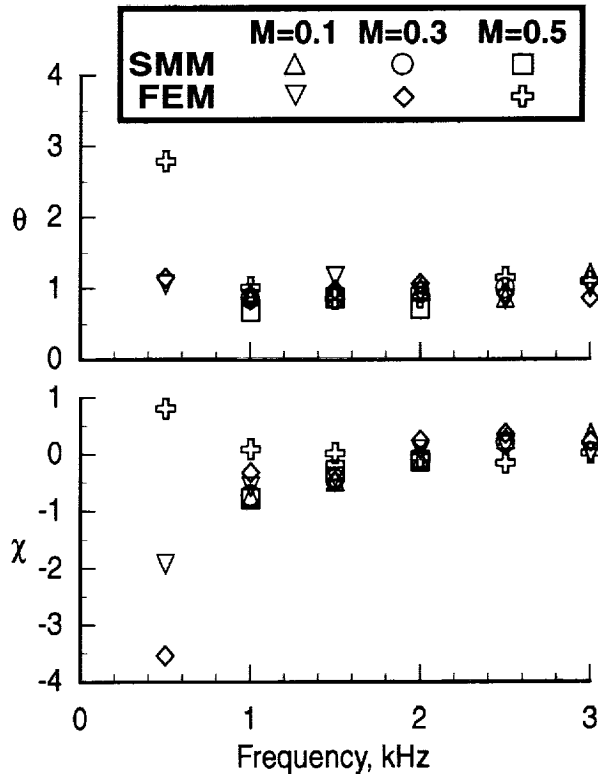


Fig. 9. Ceramic liner "CT2" with flow.

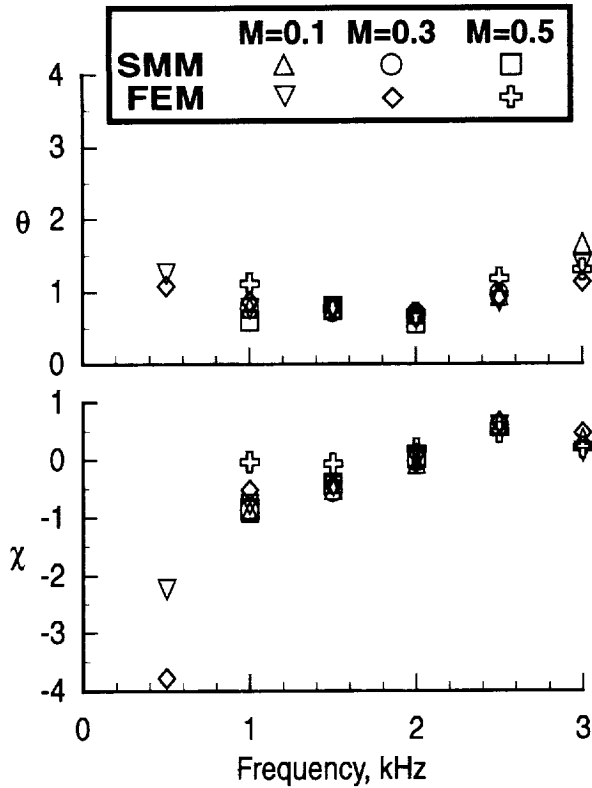


Fig. 10. Ceramic liner "CT3" with flow.

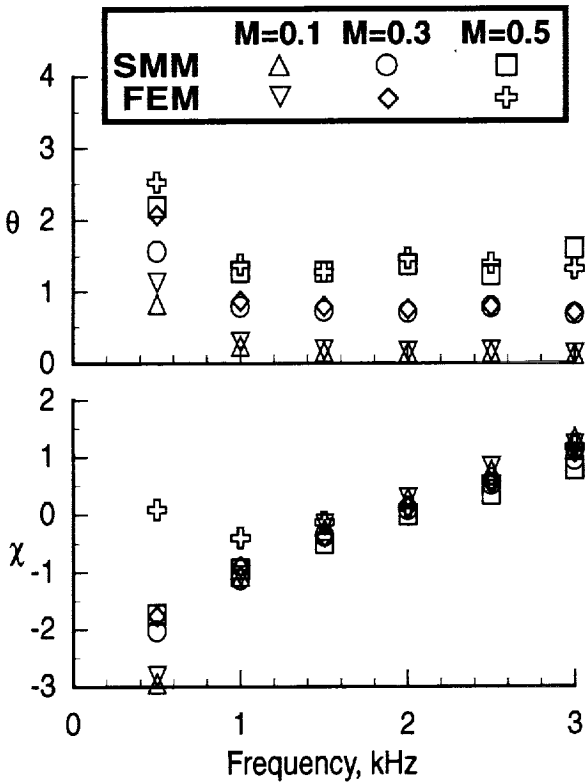


Fig. 11. Perforate liner with flow.

frequencies tested, except near the anti-resonance frequency. This difficulty at anti-resonance is typical for impedance reduction techniques.

By comparison, the impedance spectra for the "CT2" (staircase geometry) and the "CT3" (quadratic residue geometry) are relatively frequency-independent. These geometries were designed to try to achieve an acoustic resistance of unity and an acoustic reactance of zero over the entire frequency range of interest. Clearly, the impedance spectra demonstrate that the design procedure was successful. Again, as expected, all three ceramic liners are observed to be relatively insensitive to mean flow Mach number. Thus, the ceramic tubular liner results provide a useful baseline for the evaluation of acoustic waveguide methods, since the results acquired with a normal incidence impedance tube can be directly compared with those acquired with a flow impedance tube.

Finally, the impedance spectrum for the perforate liner is provided in figure 11. As expected, the acoustic resistance increases uniformly with increasing mean flow Mach number, while the acoustic reactance is relatively insensitive to changes in mean flow Mach number. Because of the separation between the acoustic resistance results for the different flow Mach numbers, the excellent comparison between SMM and FEM results is especially clear for this liner. At frequencies of 1.5 kHz and higher, the acoustic reactance is almost completely a function of the cavity depth and is virtually independent of mean flow velocity. Because of high reflections at 0.5 and 1.0 kHz, the SMM could not be implemented at a flow Mach number of 0.5. Thus, no comparisons can be made at these frequencies at Mach 0.5.

Conclusions

Based on the results of this work, the following specific conclusions are drawn:

1. In the absence of mean flow, both acoustic waveguide methods reduce impedance spectra that are almost identical with those acquired with a normal incidence impedance tube.
2. The waveguide methods confirm that impedance spectra for the ceramic tubular liners are less sensitive to mean flow effects than is the case for the perforate liner.
3. As was expected from their design features, the impedance spectra of the variable depth ceramic liners are relatively independent of frequency and mean flow velocity effects. This insensi-

tivity to flow velocity makes these liners useful for evaluation of acoustic waveguide methods.

4. When the SMM can be exercised (i.e., linear SPL and phase decay rates can be determined), it provides nearly identical impedances to those deduced with the FEM.
5. Because of its relative simplicity, the SMM should be used when the propagation data is clearly dominated by a single mode. The FEM is preferred for all other cases.

References

- ¹Phillips, B., "Effects of High Value Wave Amplitude and Mean Flow on a Helmholtz Resonator," *NASA TMX-1582*, 1967.
- ²Armstrong, D.L., Beckemeyer, R.J. and Olsen, R.F., "Impedance Measurements of Acoustic Duct Liners With Grazing Flow," Paper presented at the 87th Meeting of the Acoustical Society of America, New York, NY, 1974.
- ³Watson, W.R., Jones, M.G., and Parrott, T.L., "Validation of an Impedance Eduction Method in Flow," *AIAA Journal* Vol. 37, No. 7, 1999.
- ⁴Parrott, T.L. and Jones, M.G., "Parallel-Element Liner Impedances for Improved Absorption of Broadband Sound in Ducts," *Noise Control Engineering Journal*, 1995.
- ⁵Schroeder, M.R., "Binaural Dissimilarity and Optimum Ceilings for Concert Halls: More Lateral Sound Diffusion," *Journal of Acoustical Society of America* Vol. 65, No. 4, 1979.
- ⁶"Standard Test Method for Impedance and Absorption of Acoustical Materials Using a Tube, Two Microphones, and a Digital Frequency Analysis System," *ASTM E1050-90*, 1990.
- ⁷Jones, M.G. and Stiede, P.E., "Comparison of Methods for Determining Specific Acoustic Impedance," *Journal of Acoustical Society of America*, Vol. 101, No. 5, 1997.
- ⁸Ju, H.B. and Fung, K.-Y., "Time-Domain Impedance Boundary Conditions with Mean Flow Effects," *AIAA-2000-2003*, 2000.